CHEMISTRY
A EUROPEAN JOURNAL

DOI: 10.1002/chem.200700921

Reinforced Self-Assembly of Hexa-*peri*-hexabenzocoronenes by Hydrogen Bonds: From Microscopic Aggregates to Macroscopic Fluorescent Organogels

Xi Dou,[a] Wojciech Pisula,[a] Jishan Wu,[a] Graham J. Bodwell,[b] and Klaus Müllen*[a]

Abstract: Hexa-*peri*-hexabenzocoronene derivatives (HBCs) that have hydrogen-bonding functionalities (either amido or ureido groups) adjacent to the aromatic cores have been synthesized to study the effects of intracolumnar hydrogen bonds on the self-assembly behavior of HBCs. The hydrogen bonds effectively increased the aggregation tendency of these compounds in solution. In the bulk state, the typical columnar supramolecular arrangement of HBCs was either stabilized substantially (**1a**, **1b**, **2a**, and **2b**), or suppressed by dominant hydrogen-bonding interactions (**3**). For some of the compounds (**1a**, **2a**, and **2b**), the supramolecular arrangement adopted in the liquid-crystalline state was even retained after annealing, presumably owing to the reinforcement of the π-stacking interactions by the hydrogen bonds. Additionally, the combined effect of the hydrogen bonds and π-stacking of the aromatic moieties led to the formation of fluorescent organogels, whereby some derivatives were further investigated as novel low molecular-mass organic gelators (LMOGs).

Keywords: gels · hydrogen bonds · liquid crystals · organic gelators · pi interactions

Introduction

π Interactions have generated both theoretical[1] and experimental[2] interest in recent decades owing to their unique importance in supramolecular self-assembly behavior. Like hydrogen bonds, the strength of which ranges from 4 to 120 kJ mol^{-1},[3] π interactions (0 to 50 kJ mol^{-1}) are important secondary interactions for the construction of supramolecular architectures.[3] Because of its relatively strong and highly directional nature, hydrogen bonding has been described as the "master key interaction in supramolecular chemistry".[3] In particular, hydrogen bonds are responsible for the overall shape of many proteins, the recognition of substrates by numerous enzymes and for the double helix structure of DNA.[3] On the other hand, the comparatively weak π interactions are responsible for the slippery feel of graphite and its useful lubricant properties.[3] By combining hydrogen bonding and π interactions, it has been possible to obtain, for example, nanotubes,[4] organogels,[5] and a diversity of helical filaments[6,7] through self-assembly.

In the case of hexa-*peri*-hexabenzocoronenes (HBCs), π interactions induce columnar self-assembly and provide the basis for their distinct, intrinsic charge-carrier ability.[8] Therefore, considerable effort has been invested in the successful implementation of these and similar materials in electronic devices, such as field-effect transistors (FETs),[9]

[a] X. Dou, Dr. W. Pisula,[+] Dr. J. Wu,[++] Prof. Dr. K. Müllen
Max-Planck-Institute for Polymer Research
Ackermannweg 10, 55128 Mainz (Germany)
Fax: (+49) 6131-379-350
E-mail: muellen@mpip-mainz.mpg.de

[b] Prof. Dr. G. J. Bodwell
Department of Chemistry, Memorial University
St. John's, NL, A1B 3X7 (Canada)

[+] Present address: Degussa AG
Process Technology & Engineering
Process Technology—New Processes
Rodenbacher Chaussee 4
63457 Hanau-Wolfgang (Germany)

[++] Present address: California NanoSystems Institute
and Department of Chemistry and Biochemistry
California University at Los Angeles
607 Charles E. Young Dr. East
CA 90095–1569 Los Angeles (USA)

Supporting information for this article is available on the WWW under http://www.chemeurj.org/ or from the author. It contains MALDI-TOF and ^{1}H NMR spectra for the described compounds, additional UV-visible spectra, FTIR spectra, additional 2D WAXS patterns, additional SEM images, and LSCM pictures for the organogels.

light-emitting diodes (LEDs),[10] and photovoltaic cells.[11] The performance of the device depends, to a large extent, upon the degree of intracolumnar order of these discotic molecules in thin films, which is an important factor for efficient charge-carrier mobility.[12] The processing of such materials is a key issue in the production of well-ordered films, which can be obtained by either a thermal[13] or a solution-dependent treatment.[12,14] It has already been shown for HBCs that have carboxylic acid terminated alkyl chains that intercolumnar hydrogen bonds can strongly influence the π-mediated columnar self-assembly in the bulk state.[15]

To enhance the degree of order of discotic molecules within a single column, relatively strong and directional hydrogen bonds were brought into play through the attachment of ureido or amido groups to the HBC moieties, either directly or through rigid linkers. In so doing, it was expected that intracolumnar hydrogen bonds would form instead of the aforementioned intercolumnar hydrogen-bond networks.[15] In this context, some novel HBC derivatives that contain either amido or ureido units were synthesized (Figure 1). These functional groups are commonly used in hydrogen-bond-assisted supramolecular chemistry.[3,16] Generally, ureido groups (**2a** and **2b**) supply stronger and more rigid interactions than amido groups (**1a** and **1b**).[17] A second ureido group (**3**) was added to further enhance the interactions between the discotic molecules. The intermolecular interactions between compounds with the same kind of hydrogen-bond providers were further adapted by adjusting the size of the substituents. The self-assembly properties of these compounds in solution were investigated by electronic spectroscopy, whereas the behavior in the bulk state was examined by differential scanning calorimetry (DSC) and two-dimensional wide-angle X-ray scattering (2D WAXS) experiments.

Finally, the expectation of gel formation was realized for some of the compounds and the gelation ability of these compounds was tested in different solvent systems. Thus, a novel potential application for HBC derivatives as low molecular-mass organic gelators (LMOGs)[5] has been demonstrated.

Results

Synthesis: Monofunctionalized compounds **1a**, **1b**, **2a**, and **2b** were synthesized from **4**[18] as shown in Scheme 1. Compound **4** was treated with benzophenonimine in a Buchwald–Hartwig coupling reaction to give **5** in a yield of 95%. The hydrolysis of **5** in 2.5 M aqueous hydrochloric acid quantitatively afforded amino-substituted HBC **6** as its hydrochloride salt. Compound **6** was then treated with the corresponding acetyl chlorides or isocyanates to give compounds **1a**, **1b**, **2a**, and **2b**. Compound **3** was generated from a Hagihara–Sonogashira coupling reaction between **7** and **8**[19] in a yield of 13%. The low yield originated from the difficult workup, which was presumably a consequence of strong intermolecular hydrogen bonds.

Self-assembly behavior in solution: The way in which HBCs self-associate in solution serves as a valuable indicator for how these materials will align in films.[20] The electronic spectra of π-conjugated chromophores in solution are highly

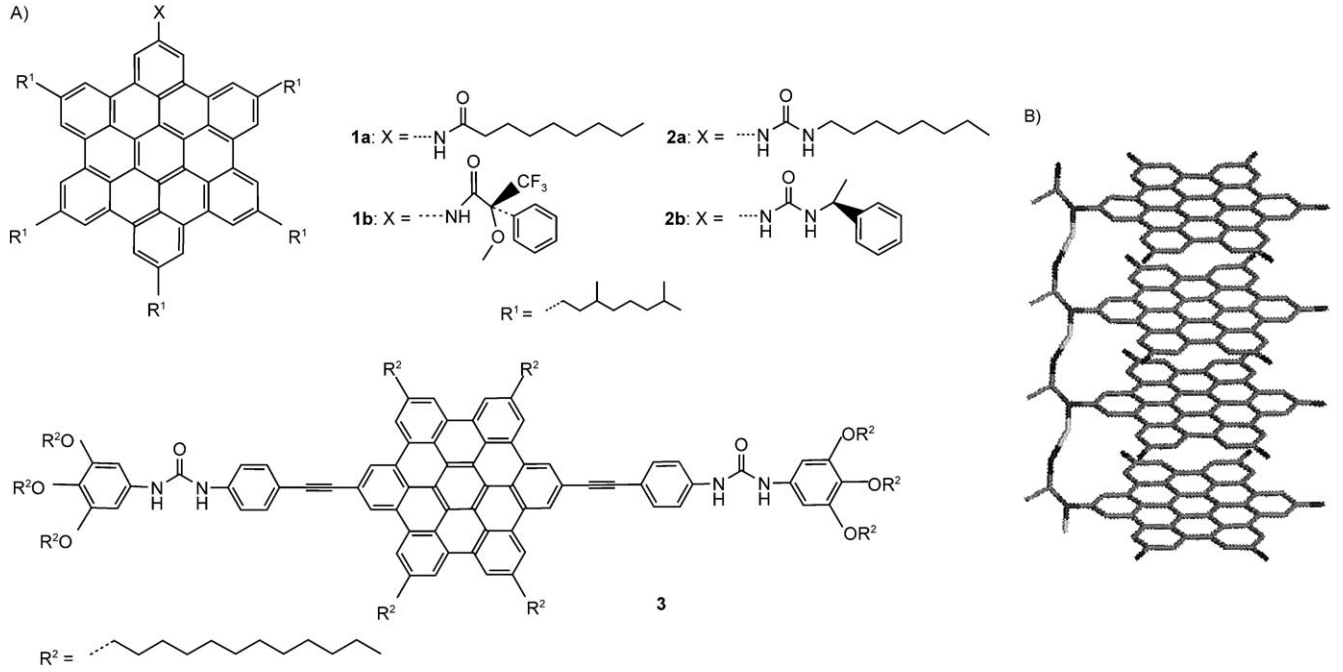

Figure 1. A) HBC derivatives that have been synthesized with amido (**1a** and **1b**) and ureido groups (**2a**, **2b**, and **3**). B) Schematic representation of the assumed intracolumnar hydrogen bonding and π-stacking interactions of monosubstituted HBC moieties.

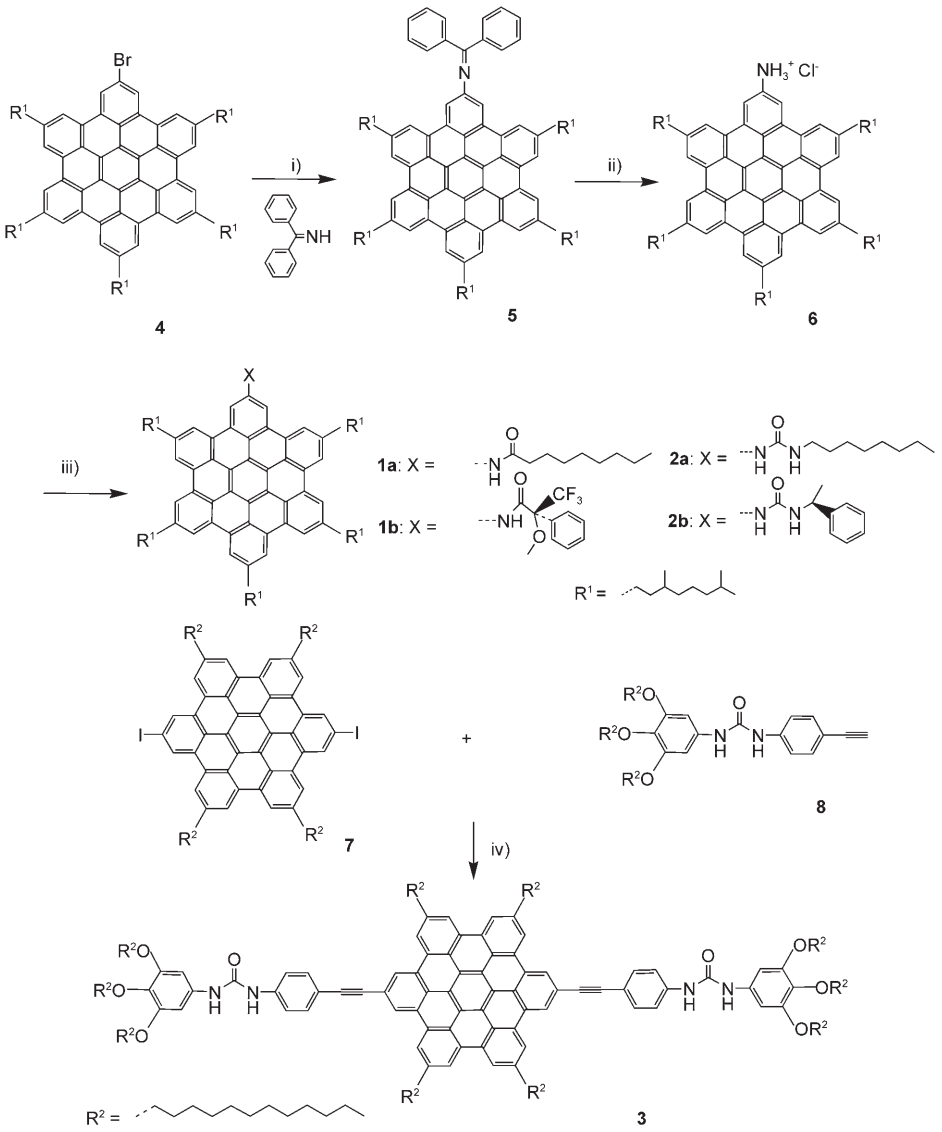

Scheme 1. Synthesis of compounds **1a**, **1b**, **2a**, **2b**, and **3**: i) $[Pd_2(dba)_3]$ (dba = dibenzylideneacetone), 2,2′-bis-(diphenylphosphino)-1,1′-binaphthyl (BINAP), $NaOC(CH_3)_3$, toluene, 80 °C, 16 h, 95 %; ii) 2.5 M HCl/THF, 5 h, 87 %; iii) appropriate acetyl chlorides or isocyanates, Et_3N, THF/toluene (1:1), 80 °C, overnight, **1a** = 88 %; **1b** = 81 %; **2a** = 60 %; **2b** = 54 %; iv) $[Pd(PPh_3)_4]$, CuI, Et_3N/THF (2:1), 50 °C, 4 d, 13 %.

sensitive to aggregational effects. For example, a variation in concentration and/or temperature can result in significant changes in the intensities, shapes, positions, and/or number of the bands.[21,22] Therefore, such investigations were conducted for all of the compounds described herein.

In contrast to the other compounds, only **2b** (Figure S6 in the Supporting Information) and **3** (Figure 2) showed distinct changes in their respective concentration-dependent UV-visible absorption spectra. With decreasing concentration, not only did the extinction coefficients of compound **3** increase substantially, but the resolution of some of the bands ($\lambda = 297$, 349, and 397 nm) also improved. Additionally, a slight blueshift of 4 nm was recorded at higher concentrations for some of the absorption bands ($\lambda = 301$ and 373 nm).

In the temperature-dependent absorption spectra of the monofunctionalized HBCs, compound **2b** exhibited the most pronounced effects. Compounds **1a** (Figure 3A) and **2a** (Figure S7B in the Supporting Information) showed similar, but less-pronounced effects, whereas **1b** did not display any recognizable change (Figure S7A in the Supporting Information). Upon increasing the temperature of solutions of **1a** (Figure 3A) and **2b** (Figure 3B), the resolution of the absorption bands at shorter wavelengths improved and some broad bands at longer wavelengths (approximately 410–420 nm) became less intense with the appearance of an isosbestic point at around 400 nm. Moreover, the α bands (named according to Clar's nomenclature[23]), which are generally very weak for HBC derivatives,[24] were also much better resolved at higher temperatures.

Significant changes were also observed in the temperature-dependent UV-visible absorption spectrum of **3** (Figure 4), in which two isosbestic points were apparent (at 349 and 389 nm). For the bands at about 300 nm and those at longer wavelengths, the intensity decreased with increasing temperature, whereas the band between the isosbestic points changed in the opposite sense.

The fluorescence spectra of **2a**, **2b**, and **3** varied with increasing concentration (Figure 5A). In particular, the bands at longer wavelengths became more intense and broader.

Compounds **1b** and **2b** each have one chiral center in the functional substituent. Circular dichroism (CD) spectroscopy revealed weak Cotton effects for **1b**, but not **2b**, presumably owing to the size of the molecule in relation to the number of chiral centers.

Hydrogen-bonding interactions and self-assembly behavior in the bulk state: Infrared spectroscopy of the bulk state samples supported the formation of hydrogen bonds in

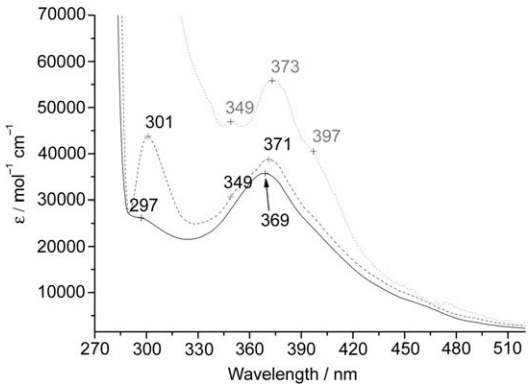

Figure 2. Concentration dependent UV-visible absorption spectra of **3** in solution in toluene for 1.56×10^{-5} (——), 1.56×10^{-6} (-----), and 1.56×10^{-7} M (•••••).

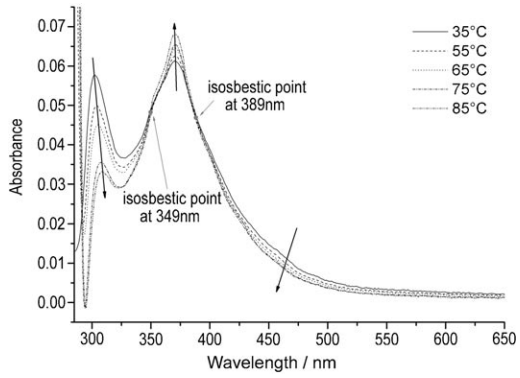

Figure 4. Temperature-dependent UV-visible absorption spectra of **3**, measured in solution in toluene (1.56×10^{-6} M); arrows indicate the direction of change with increasing temperature.

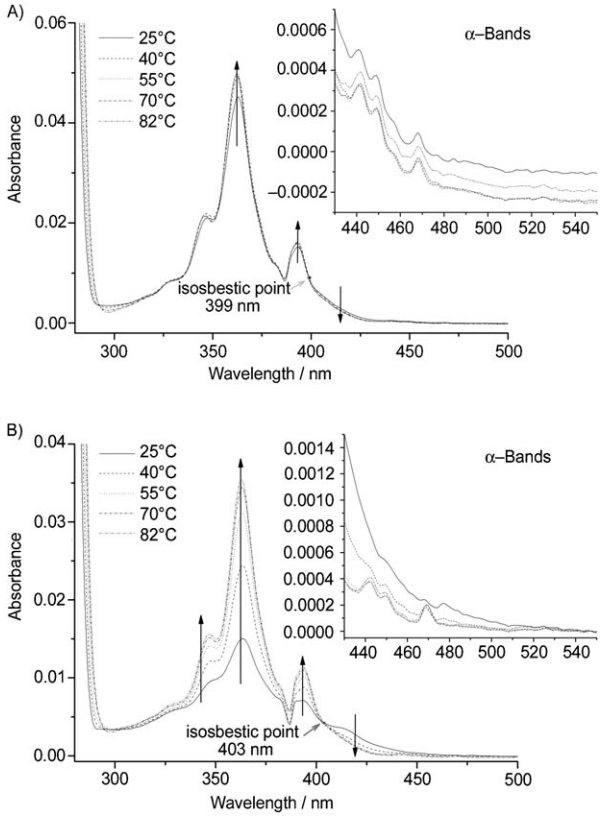

Figure 3. Temperature-dependent UV-visible absorption spectra of **1a** (A) and **2b** (B) measured in solution in toluene (1.0×10^{-5} M); arrows indicate the direction of change with increasing temperature.

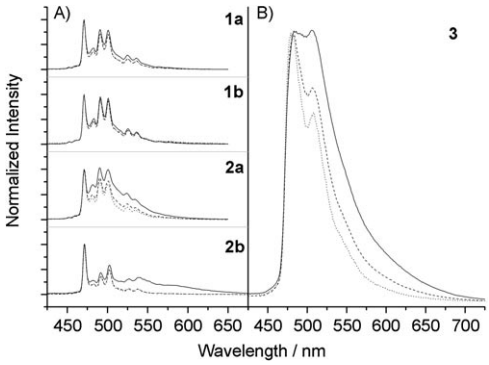

Figure 5. Concentration-dependent fluorescence spectra of **1a**, **1b**, **2a**, **2b** (A) and **3** (B) in toluene at 10^{-5} (——), 10^{-6} (-----), and 10^{-7} M (•••••); excited at 360 nm and normalized at 471 nm for **1a**, **1b**, **2a**, and **2b**; excited at 369 nm and normalized at 482 nm for **3**.

Table 1. Stretching frequencies [cm^{-1}] of N–H ($\tilde{\nu}_{N-H}$) and carbonyl ($\tilde{\nu}_{C=O}$) groups of compounds **1a**, **1b**, **2a**, **2b** and **3** in KBr pellet.

Compound	$\tilde{\nu}_{N-H}$ [cm^{-1}]	$\tilde{\nu}_{C=O}$ [cm^{-1}]
1a	3430 (medium, broad)	1660 (medium)
	3310 (shoulder)	
1b	3400 (medium, broad)	1700 (medium)
2a	3430 (medium, broad)	1710 (medium)
	3310 (shoulder)	1650 (weak)
2b	3390 (medium, broad)	1640 (medium)
	3310 (medium, broad)	
3	3310 (medium, broad)	1650 (medium)

these compounds according to the distinct changes induced in the vibrational frequency of the N–H and carbonyl groups.[25]

The characteristic stretching vibrations of the N–H bond and the carbonyl group are listed in Table 1 (see Figure S8 in the Supporting Information for full spectra). For secondary amide and urea compounds, which involve hydrogen bonds, the characteristic N–H stretching vibrations usually give multiple bands in the range of $\tilde{\nu}_{N-H}=3400$–$3060\ cm^{-1}$ and the carbonyl stretching vibrations, so-called amide I bands, appear at lower frequencies ($\tilde{\nu}_{C=O}=1700$–$1640\ cm^{-1}$) in contrast to a saturated aliphatic ketone ($\tilde{\nu}=1715\ cm^{-1}$) owing to the resonance effect.[25a] For compounds **1b**, which has a sterically hindered amido functionality, and **3**, which has two ureido groups, only one kind of N–H and carbonyl

stretching bands were recorded. Specifically, both the N–H and the carbonyl stretching bands for **1b** were located at relatively higher wavenumbers than those for **3**. The other compounds all had two kinds of N–H stretching bands and **2a** even had two carbonyl stretching signals.

DSC is a method commonly used for investigating thermotropic phase behavior and gives information about phase-transition temperatures and the corresponding enthalpies.[26] For **1a**, **1b**, and **3**, there was no visible phase-transition peak recorded in the temperature range from −100 to 250 °C. In the case of **2b**, the DSC trace showed only an irreversible endothermic transition at 220 °C during both the first and second heating cycles.

2D WAXS experiments,[27] which provide information about the supramolecular arrangement in the solid state, were conducted for all of the compounds at both ambient and elevated temperatures. Compounds **1a**, **2a**, and **2b** exhibited similar phase behavior. Figure 6 presents the temperature-dependent 2D WAXS patterns of **1a** and **2b** (for **2a** see Figure S9 in the Supporting Information). At 30 °C, the characteristic distribution of the reflections indicated identical monoclinic columnar stacking for both compounds.[27] From the meridional and off-meridional scattering intensities, it was determined that the discotic molecules were tilted by approximately 40°, the columnar axis had a periodic distance of 0.47 nm, and the π-stacking distance was 0.37 nm.[27a]

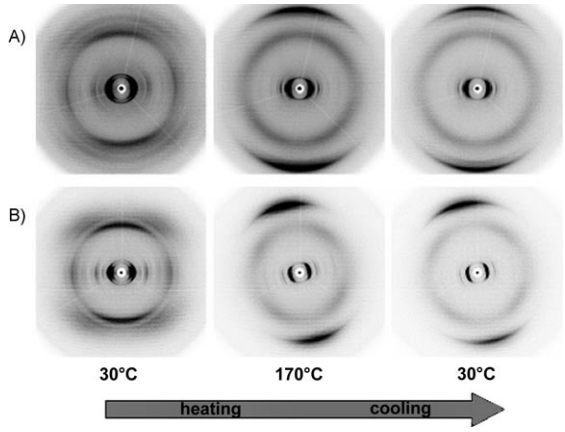

Figure 6. Temperature-dependent 2D WAXS experiments of A) **1a** and B) **2b**; 2D monoclinic unit cell parameters (at 30 °C): $a=2.46$, $b=1.93$ nm; $\gamma=115°$ for **1a** and $a=2.50$, $b=1.86$ nm; $\gamma=95°$ for **2b**; hexagonal unit cell parameters (at 170 °C and after annealing): $a_{hex}=2.77$ nm for **1a** and $a_{hex}=2.80$ nm for **2b**.

Upon heating to 170 °C, the 2D patterns of both compounds (Figure 6) displayed a typical liquid-crystalline (LC) arrangement of the molecules,[27] in which the discs self-arranged perpendicular to the columnar axis with a stacking distance of 0.37 nm in a hexagonal columnar lattice. Interestingly, upon cooling the samples to room temperature after about one hour at 170 °C, the highly ordered LC organization did not return to the crystalline phase previously recorded (as observed for other alkylated disk-type PAHs),[28] but rather retained the nontilted, hexagonal 2D packing observed in the mesophase.

Compound **3** showed significantly less order over the entire temperature range, which rendered the assignment of a unit cell impossible. At room temperature, no π-stacking signal was observed. At 120 °C, meridional reflections were apparent, which correspond to a cofacial stacking distance of 0.38 nm. The π–π distance decreased to a typical aromatic stacking value of 0.36 nm at 180 °C. In contrast to the behavior observed for **1a**, **2a**, and **2b**, the LC organization at higher temperatures was not retained after annealing (Figure S10 in the Supporting Information). Unlike the above-mentioned derivatives, **1b** showed nontilted, hexagonal columnar stacking ($a_{hex}=2.58$ nm) with a cofacial distance of 0.36 nm over the whole temperature range investigated (Figure S11 in the Supporting Information).

Gelation ability test: For initial gelation testing, attempts to dissolve each of the compounds in a small amount of an apolar solvent (e.g., hexane, heptane, or toluene) at reflux temperatures were made. THF was then progressively added as a polar solvent if a particular compound did not dissolve under the initial conditions. The solution was then slowly cooled (by placing it in a 60 °C oil bath and allowing the oil bath to cool to ambient temperatures) and the substance was judged to be a gel if the vessel could be inverted without apparent movement of the content.[17] The minimum gelation concentration, which describes the gelation ability of the compounds, was determined by continuously diluting a gel (with the same solvent mixture as the one used to form the gel) with heating and cooling cycles until the gel did not regenerate. Another important parameter of gels, the so-called sol-to-gel phase-transition temperature (T_g), which describes their thermodynamic stability, was measured by using the falling-drop method.[29]

The efficient combination of hydrogen bonding and π interactions led to distinct gelation properties for two of the compounds (**2b** and **3**). Only these two examples developed stable fluorescent organogels (Figure 7A) in the solvents tested. The minimum gelation concentrations are shown with the corresponding T_g values in Table 2. Laser scanning

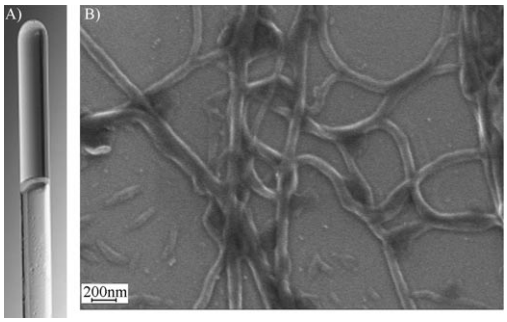

Figure 7. A) Photograph of fluorescent gel from **3** in toluene. B) SEM image of xerogel prepared from **2b** in hexane/THF.

Table 2. Gelation test for **2b** and **3** in *n*-hexane/THF, *n*-heptane/THF, and toluene/THF.

	Apolar solvent[a] [mL]	THF [mL]	$G.C._{min}$[b] [wt%]	Phase/ T_g [°C]
hexane				
2b[c]	0.55	1.30	0.068	G[d]/43
heptane				
2b[c]	0.60	1.10	0.081	G/31
toluene				
2b[c]	0.50	0.35	0.15	G/A[e]
3[f]	1.90	0	0.035	G/42

[a] Hexane, heptane, or toluene. [b] $G.C._{min}$ = minimum gelation concentration. [c] 1 mg vol^{-1}. [d] G = gel at room temperature; [e] A = destroyed by mechanical agitation. [f] 0.6 mg vol^{-1}

confocal microscopy (LSCM) indicated that the fluorescence comes from the fibrillar structure itself and not from amorphous material (Figure S19 in the Supporting Information).

To visualize how the nanoscale hydrogen-bonding interactions manifest themselves in the macroscopic superstructures, a scanning electron microscopy (SEM) image of a xerogel of **2b** was recorded (Figure 7B).[30] The molecules aggregated into long fibrillar structures (up to several microns in length) with a diameter of approximately 100 nm. These fibers further interwound with each other to establish three-dimensional networks, which are the only known examples for HBC derivatives (for more SEM pictures, see Figures S20A and B for **2b** and C and D for **3** in the Supporting Information).

Discussion

As indicated by the results, the presence of hydrogen bonds strongly influenced not only the solution behavior, but also the bulk properties of the HBC derivatives. In solution, the non-Lambert–Beer law behavior and the concentration dependence of the absorption spectra (sharp, well-resolved band shape with larger extinction coefficients at lower concentrations) indicated the existence of larger aggregates at higher concentrations.[13c] The slight blueshift of one of the absorption bands (from 373 to 369 nm) in the spectrum of **3** was also consistent with cofacial stacking of the aromatic π-systems in the aggregates.[13a,31b] This phenomenon has been studied both theoretically and experimentally.[31] The existence of increasing aggregation with increasing concentration for **2a**, **2b**, and **3** was further supported by concentration-dependent fluorescence experiments, which exhibited broad, less-resolved concentration-dependent bands above 500 nm. The less-pronounced photophysical changes in **1a** and **1b** indicated lower self-association propensities, which are likely to be as a result of the weaker hydrogen-bonding interactions between amido functionalities than ureido groups.[17]

As the aromatic moieties of compounds **1a**, **1b**, **2a**, and **2b** consist of the same basic structure, very little difference in the strength of the π interactions can be expected. Therefore, the different self-assembling abilities can be attributed to the differences in the degree of hydrogen bonding,[16,17a] which is strongly influenced by the temperature,[32] the steric demands of the side chains attached to the hydrogen bonding groups, and the number of hydrogen-bonding functionalities. Concerning the influence of temperature, regardless of the nature of the hydrogen-bonding group, the effects were effectively suppressed upon moderate heating, as indicated by the close similarity of the absorption spectra at 82 °C and their marked differences at 25 °C (Figure 3 and Figure S7 in the Supporting Information). Superimposed upon the temperature effect was a steric effect. Specifically, the spectrum of **1b**, which carries the bulkiest side chain (the 2-(*R*)-(−)-α-methoxy-α-(trifluoromethyl)phenylethylamido group), showed very little changes with respect to temperature variation (Figure S7A in the Supporting Information). In contrast, the spectrum of **1a**, which has a less bulky appendage, displayed more pronounced changes (Figure 3A). The dominant effect is the nature of the hydrogen-bonding group. The spectra of the ureido-containing HBCs (**2a** and **2b**; Figures S7B and 3B in the Supporting Information) exhibit much greater temperature dependence than those of the amido-containing HBCs (**1a** and **1b**). The number of hydrogen-bonding groups present also played a significant role, as demonstrated by the strong temperature dependence observed in the spectrum of **3** (two ureido groups). In this case, the spectrum was still changing at the upper temperature limit (85 °C), which indicated that hydrogen-bonding interactions had not yet been suppressed.

In the CD spectrum of **1b** (Figure S21 in the Supporting Information), the Cotton effects are quite weak. However, the pattern observed is consistent with a clockwise helical aggregation of molecular dipole moments in solution.[33] The SEM image of the xerogel prepared from **2b**, which showed no CD signal, appeared to show discernable left-handed helical structures in the gel fibers of **2b** (Figure S20A in the Supporting Information).

In the bulk state, the differences in the degree of hydrogen-bonding interactions also became obvious. The observation of multiple N–H stretching vibrations for **1a**, **2a**, and **2b** in their FTIR spectra (Table 1, Figure S8 in the Supporting Information) suggested that the amido/ureido groups might bind to produce dimers with an *s-cis* conformation or polymers with an *s-trans* conformation.[25a] When comparing the two amido-containing compounds (**1a** and **1b**), the carbonyl stretching of **1a** was observed at a frequency that was 40 cm^{-1} lower than that of **1b**, which suggested the existence of stronger hydrogen bonds in **1a**. Among the ureido-containing compounds, compounds **2b** and **3** gave only one carbonyl stretching signal ($\tilde{\nu}$ = 1640 (**2b**) and 1650 cm^{-1} (**3**)), whereas two carbonyl stretching bands were observed for **2a** ($\tilde{\nu}$ = 1710 and 1650 cm^{-1}). This result may be a reflection of different hydrogen-bonding interactions in these three compounds.[34] These observations are in agreement with the results obtained from solution studies that **1b**, which has a bulky amido substituent, formed the weakest hydrogen bonds and that hydrogen bonding was significantly strength-

ened both by reducing the size of the substituent and by using a more effective hydrogen-bonding ureido group.

The supramolecular columnar arrangements of the compounds at different temperatures were investigated by 2D WAXS, whereby it was found that the hydrogen-bonding interactions strongly influenced the stacking and especially the thermal properties of these materials. The most interesting observation was the irreversibility of mesophase formation after annealing for compounds **1a**, **2a**, and **2b**, which is a unique property for HBC derivatives. The columnar stacking at room temperature before annealing resembled that of most other HBC molecules in the crystalline phase.[27a] The periodic distance along columns was determined to be 0.47 nm for **1a** and **2b**, and 0.46 nm for **2a**, which is in good agreement with the length of the hydrogen-bonding units between the urea and amide groups (0.44–0.48 nm).[16,17a,35] This provides the opportunity for a near-optimum arrangement of hydrogen-bonding functional groups. As the temperature was increased to 170 °C, the effect of the hydrogen bonds was weakened and π interactions became the dominant influence on the supramolecular arrangement. This led to a typical LC organization with nontilted molecular discs, a typical intermolecular π-stacking distance (0.36 nm), and hexagonal 2D columnar packing. Thereby, stacked arenes separated by 0.36 nm and hydrogen bonds of 0.47 or 0.46 nm can be simultaneously accommodated in the structure shown in Figure 8, which has a helical arrangement. The unexpected preservation of the LC supramolecular organization after prolonged annealing is consistent with the observation of only an irreversible endothermic transition during the heating cycle on the DSC diagram (**2b**). This behavior can be explained in terms of the relative importance of various weak interactions at different temperatures. At low temperatures, the hydrogen bonding and the crystallinity of the alkyl substituents dictate the supramolecular arrangement to give monoclinic columnar packing with tilted molecular discs. At high temperatures, the relative importance of hydrogen bonding lessens[32] and π interactions become dominant. As such, a hexagonal columnar arrangement forms. Upon cooling, the order imposed by π stacking remains in place and intermolecular hydrogen bonding between side chains cements the structure. Thus, the cooperative effects of the weak interactions (π stacking, hydrogen bonding, and side chain crystallinity) are responsible for the preservation of the LC phase. Again, it is noteworthy that the functional groups are attached directly to the aromatic cores and the intracolumnar hydrogen bonds are thus established between discs within the same supramolecular column. This stands in stark contrast to the previously reported HBC derivatives, which had hydrogen-bonding functionalities that were separated from the HBC cores by long alkyl spacers and resulted in the formation of intercolumnar hydrogen bonds.[15]

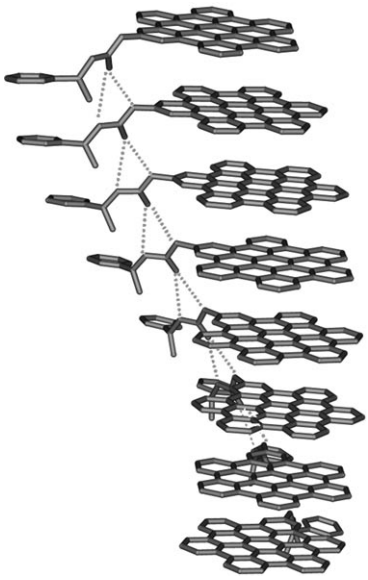

Figure 8. Schematic representation of the coincidence of hydrogen-bonding interactions and π interactions after annealing for **2b**.

The observation that **1b** maintained the same columnar arrangement over the whole temperature range suggested a less pronounced influence of hydrogen bonds on the supramolecular arrangement at low temperatures.

Upon inclusion of a second ureido group (i.e., **3**), the 2D WAXS pattern revealed an increased disorder at low temperatures, which implied an even stronger influence of the hydrogen bonds. The decrease in the cofacial stacking distance (from 0.38 to 0.36 nm) upon increasing the temperature (from 120 °C to 180 °C) showed that the supramolecular arrangement induced by the π interactions could only be obtained after the hydrogen bonds were significantly weakened at higher temperatures. The loss of long range order upon cooling not only indicates that hydrogen bonding is more important than π interactions at room temperature, but also that the two effects do not operate cooperatively in this system.

All of the results discussed above clearly demonstrate that for successful cooperative implementation of two secondary forces to improve the self-assembling propensity, the spatial demands and geometrical requirements need to coincide. By selecting a stronger hydrogen-bond donor, that is, the ureido unit, and reducing the size of the side chain attached to the functional group, for example, as in **2b**, the HBC derivative exhibited excellent self-assembling ability both in solution and in the solid state. The introduction of a second strong hydrogen-bond provider at the *para* position (in the case of **3**) was, however, counterproductive. A bulky side chain and relatively feeble hydrogen-bonding group, in the case of **1b**, resulted in an almost undetectable influence on the self-assembly behavior of the HBCs.

It has been observed previously that amphiphilic HBCs are capable of gelling some organic solvents under certain conditions.[36] For compounds **2b** and **3**, the combination of stronger and more rigid hydrogen bonds and their intrinsic π interactions caused the HBCs to behave like LMOGs. Both materials exhibited excellent gelation abilities with very low minimum gelation concentrations compared with

perylene-[37] and porphyrin-based[17c,d,35g] LMOGs, which also combine π interactions with hydrogen bonds. The gelling process could be assumed to be as follows: The hydrogen bonds were initially significantly weakened in solution by heating at reflux and the π interactions dominated the molecular aggregation. As in the bulk state, the hydrogen-bonding interactions stabilized these aggregates upon cooling and further accumulated these microscopic aggregates into fibrillar supramolecular structures. An SEM image of the xerogel (Figure 7B) showed that the resulting three-dimensional network trapped small solvent molecules and stabilized the substance in a metastate between liquid and solid, which led to the formation of fluorescent organogels.

Conclusion

Through the introduction of hydrogen bonds along the HBC columnar axis, the self-association propensities of HBC derivatives have been improved considerably and were also strongly influenced by varying both the size of the substituents and the nature of the hydrogen-bonding groups at the same time. The self-assembling abilities of these compounds increased substantially as the hydrogen-bonding interactions became stronger and the steric demands of the side chains diminished. Accordingly, the compound with the weaker hydrogen-bonding group and the bulkier substituent (**1b**) exhibited the lowest aggregation tendency. By the same token, either reducing the steric hindrance of the substituent (**1a**) or incorporating a stronger hydrogen-bonding unit (**2a**, **2b**) endowed the HBCs with a stronger self-assembling ability. When a second hydrogen-bond donating group was connected to the aromatic core at the *para* position (**3**), the molecule displayed the strongest aggregation tendency in solution.

Nevertheless, in the bulk state, depending upon the strength of the intermolecular interactions and the geometry of functional groups, hydrogen bonds either cooperated with the π interactions to stabilize the HBC columnar superstructures, which even resulted in the preservation of a highly ordered LC phase after annealing (**1a**, **2a** and **2b**), or competed against the π interactions, which led to a short-range ordered supramolecular arrangement (**3**).

Finally, the relatively stronger hydrogen bonds of **2b** and **3** rendered these HBC derivatives as LMOGs, which has never been characterized previously for HBC derivatives. HBC molecules **2b** and **3** assembled into stable, three-dimensional networks under the collaboration of hydrogen bonding and π interactions, which trap small solvent molecules to form fluorescent organogels. The hydrogen bonds significantly enhanced the self-assembling abilities of the HBCs and thus endowed them with excellent gelation abilities. In so doing, the optoelectronic properties of HBCs have been made available for exploitation in the area of functional organogels. Owing to the intrinsic semiconducting properties of stacked HBCs, such gels are promising candidates for applications in areas such as energy transfer along one-dimensional aligned chromophores,[17d,38a] enhanced charge transport based on organic semi-conducting layers,[38b] light-scattering electrooptical materials through the cooperation of LC moieties,[38c] and sensor devices[6,38d] (following the introduction of additional functionalities).

Experimental Section

General methods: Chemicals were obtained from Fluka, Aldrich, and ABCR and used as received. Column chromatography and TLC were performed with Merck silica gel 60 (70–230 mesh) and Merck silica gel 60 F254, respectively. ^{1}H NMR and ^{13}C NMR spectra were recorded by using a Bruker DPX 250, Bruker 300 AMX, Bruker DRX 500, or Bruker DRX 700 spectrometer with the solvent proton or carbon signal as an internal standard. MALDI-TOF mass spectra were measured by using a Bruker Reflex II-TOF spectrometer with a 337 nm nitrogen laser and 7,7,8,8-tetracyanoquinodimethane (TCNQ) as the matrix. The optical absorption measurements were performed at ambient temperatures by using a UV/Vis/NIR Perkin–Elmer Lambda 900 spectrometer. The photoluminescence in solution was recorded by using a SPEX Fluorolog 2 type 212 steady-state fluorometer. Infrared spectroscopy was measured by using Nicolet FTIR 320 spectrometer. DSC measurements were conducted by using a mettler DSC 30 instrument with a heating and cooling rate of 10 °C min^{-1}. The 2D-WAXS experiments were performed by means of a rotating anode (Rigaku 18 kW) X-ray beam with a pinhole collimation and a 2D Siemens detector. A double graphite monochromator for the $Cu_{K\alpha}$ radiation ($\lambda = 0.154$ nm) was used. Electron microscopy was performed by using a Zeiss 1530 electron microscope. LSCM was conducted by using a LSM 510 laser scanning module coupled to a Zeiss Axiovert 200 M inverted microscope.

2-Benzophenonimino-5,8,11,14,17-penta(3,7-dimethyloctanyl)hexa-*peri*-hexabenzocoronene (5): 2-Bromo-5,8,11,14,17-penta(3,7-dimethyloctanyl)hexa-*peri*-hexabenzocoronene (**4**) (261.3 mg, 201.0 mmol), [$Pd_2(dba)_3$] (4.9 mg, 5.0 mmol), BINAP (10.0 mg, 16.0 mmol), and sodium *tert*-butoxide (461.0 mg, 4.8 mmol) were dissolved in dry toluene (10 mL) and heated to 80 °C in a 25 mL Schlenk flask under argon. Then benzophenonimene (870.0 mg, 4.8 mmol) was added dropwise. The mixture was stirred at 80 °C for 16 h. After cooling, the mixture was poured into methanol (100 mL). The yellow solid that precipitated was filtrated, redissolved in a minimum amount of THF and precipitated by adding methanol twice. Compound **5** was obtained as yellow solid (265 mg, 95 %). ^{1}H NMR (250 MHz, $CDCl_3$, 25 °C): $\delta = 8.30$–8.26 (m, 6H; Ar–H), 8.16–8.12 (m, 6H; Ar–H), 7.60–7.59 (m, 4H; Ar–H), 7.40–7.37 (m, 2H; Ar–H), 7.20–7.11 (m, 4H; Ar–H), 3.04–2.90 (m, 10H; α-CH_2), 1.98–1.14 (m, 65H; −CH, −CH_2, −CH_3), 0.92–0.90 ppm (m, 30H; −CH_3); ^{13}C NMR (62.5 MHz, [D_8]THF, 25 °C): $\delta = 168.1$, 148.9, 141.2, 140.8, 140.7, 140.6, 138.0, 131.6, 130.9, 130.6, 130.5, 130.4, 130.3, 129.4, 129.1, 129.0, 123.8, 123.7, 123.6, 122.3, 121.9, 121.7, 120.0, 119.9, 119.8, 116.2, 41.1, 41.0, 40.5, 38.6, 38.5, 35.8, 34.4, 29.1, 23.3, 23.2, 20.4 ppm; MS (MALDI-TOF, TCNQ): *m*/*z* (%): 1404 (100 %) $[M+H]^+$.

2-Amino-5,8,11,14,17-penta(3,7-dimethyloctanyl)hexa-*peri*-hexabenzocoronene hydrochloride (6): Compound **5** (297.3 mg, 0.2 mmol) was dissolved in THF (10 mL) and 2.5 M HCl (70 mL) was added under an argon atmosphere. The solution immediately, but temporarily, turned black followed by the formation of a suspension of yellow powder in the aqueous solution. The mixture was stirred vigorously for 5 h and filtered. The solid was washed with water until the pH value of the filtrate was close to 7, then it was washed with acetone to remove excess diphenylketone, as monitored by TLC. Ammonium salt **6** was collected as a yellow powder after being dried under high vacuum (236 mg, 87 %). MS (MALDI-TOF, TCNQ): *m*/*z* (%): 1239 (100 %) $[M-H]^+$. This compound was used directly in the next step, owing to the instability of the free base. NMR spectroscopy was not used for structural characterization, but rather the spectra of derivatives were measured.

General procedure for the synthesis of compounds 1a and 1b: Compound **6** (0.06 mmol, 74.3 mg), triethylamine (0.5 mL) and LiBr (110.0 mg) were added to a mixture of toluene/THF (1:1, 5 mL) and heated to 80 °C under an argon atmosphere. The appropriate acetyl chloride (0.6 mmol) was added dropwise. The mixture was stirred at 80 °C overnight. After cooling to room temperature, the mixture was poured into methanol (100 mL). The precipitate was collected and further purified by column chromatography.

2-Nonylamido-5,8,11,14,17-penta(3,7-dimethyloctanyl)hexa-peri-*hexabenzocoronene (**1a**)*: Compound **1a** was prepared according to the general procedure. The product was purified by using a silica gel column and a mixture of low-boiling petroleum ether/CH_2Cl_2 (2:1) as the eluent (R_f = 0.36) to afford **1a** as a yellow powder (79 mg, 88 %). ^{1}H NMR (250 MHz, [D$_8$]THF/LiBr, 50 °C): δ = 10.91 (s, 1H; −NH), 9.32 (s, 2H; Ar−H), 8.47 (s, 2H; Ar−H), 8.36 (s, 2H; Ar−H), 8.27–8.19 (m, 6H; Ar−H), 3.05–2.96 (m, 12H; α-CH_2), 2.01 (br s, 12H; β-CH_2), 1.57–1.15 (m, 65H; −CH, −CH_2), 0.96–0.88 ppm (m, 33H; −CH_3); ^{13}C NMR (62.5 MHz, [D$_8$]THF/LiBr, 50 °C): δ = 173.3, 146.3, 140.8, 140.3, 140.2, 138.9, 135.7, 130.8, 130.6, 130.4, 130.2, 130.0, 129.9, 125.9, 123.7, 123.5, 122.4, 121.7, 121.6, 121.4, 119.9, 119.6, 119.5, 119.4, 114.6, 41.0, 40.9, 40.5, 38.5, 34.4, 34.3, 32.8, 31.8, 31.0, 30.9, 30.5, 29.0, 23.2, 23.1, 20.3, 14.4 ppm; MS (MALDI-TOF, TCNQ): *m*/*z* (%): 1379 (100 %) [*M*]$^+$.

*2-(*R*)-(−)-α-methoxy-α-(trifluoromethyl)phenylethylamido-5,8,11,14,17-penta(3,7-dimethyloctanyl)hexa*-peri-*hexabenzocoronene (**1b**)*: Compound **1b** was prepared according to the general procedure. The product was purified by using a silica gel column and a mixture of low-boiling petroleum ether/THF (10:1) as the eluent (R_f = 0.56) to afford **1b** as a yellow powder (72 mg, 81 %). ^{1}H NMR (250 MHz, [D$_8$]THF, 25 °C): δ = 10.01 (s, 1H; −NH), 9.57 (s, 2H; Ar−H), 8.77 (br s, 4H; Ar−H), 8.69 (s, 2H; Ar−H), 8.63–8.61 (m, 4H; Ar−H), 7.96 (d, ^3J(H,H) = 7.2 Hz, 2H; Ar−H), 7.57–7.53 (m, 3H; Ar−H), 3.90 (s, 3H; −OCH_3), 3.29–3.19 (m, 10H; α-CH_2), 2.01–1.21 (m, 68H; −CH, −CH_2), 0.93–0.91 ppm (m, 33H; −CH_3); ^{13}C NMR (175 MHz, [D$_8$]THF, 25 °C): δ = 168.8, 144.5, 144.3, 144.2, 140.4, 137.8, 134.7, 133.9, 133.7, 133.6, 127.2, 126.9, 126.1, 123.3, 123.1, 116.9, 44.1, 43.9, 43.5, 41.5, 38.8, 38.7, 37.3, 37.2, 33.6, 32.0, 26.2, 26.1, 23.3 ppm; MS (MALDI-TOF, TCNQ) *m*/*z* (%): 1455 (100 %) [*M*]$^+$.

General procedure for the synthesis of compounds 2a and 2b: Compound **6** (123.9 mg, 0.1 mmol), LiBr (55 mg), and triethylamine (0.5 mL) were added to a mixture of toluene/THF (1:1, 5 mL) and heated to 80 °C under argon. The appropriate isocyanate (1.3 mmol) was added dropwise, and the reaction stirred at 80 °C for 45 h. After the mixture was cooled, the crude product was precipitated in methanol (250 mL) and dried under vacuum after filtration. The crude product was further purified by column chromatography.

*2-(*N′*-Octanylureido)-5,8,11,14,17-penta(3,7-dimethyloctanyl)hexa*-peri-*hexabenzocoronene (**2a**)*: Compound **2a** was prepared according to the general procedure. The product was purified by using a mixture of low-boiling petroleum ether/CH_2Cl_2 (3:1) with LiBr and then LiBr/THF as the eluents (R_f = 0.4) to afford **2a** as a brown solid (75 mg, 60 %). ^{1}H NMR (250 MHz, [D$_8$]THF/LiBr, 50 °C): δ = 9.81 (s, 1H; −NH), 8.97 (br s, 2H; Ar−H), 8.64 (s, 2H; Ar−H), 8.41–8.17 (m, 8H; Ar−H), 7.59 (s, 1H; −NH), 3.41 (br s, 2H; α-CH_2), 3.13–3.05 (m, 10H; α-CH_2), 2.17–1.83 (m 12H; β-CH_2), 1.65–1.14 (m, 65H; −CH, −CH_2), 0.95–0.82 ppm (m, 33H; −CH_3); ^{13}C NMR (175 MHz, [D$_8$]THF/LiBr, 50 °C): δ = 160.8, 144.5, 144.6, 144.3, 144.2, 135.8, 133.6, 126.9, 126.6, 125.7, 125.3, 125.1, 123.6, 123.3, 122.6, 44.7, 44.3, 44.2, 43.8, 43.6, 41.6, 38.8, 38.6, 37.5, 37.4, 37.2, 36.1, 35.9, 33.9, 33.8, 33.7, 33.5, 33,4, 33,3 32.1, 31.2, 23.4, 17.5 ppm; MS (MALDI-TOF, TCNQ): *m*/*z* (%): 1394 (100 %) [*M*]$^+$.

*2-(*N′*-(S)-(−)-1-phenylethylureido)-5,8,11,14,17-penta(3,7-dimethyloctanyl)hexa*-peri-*hexabenzocoronene (**2b**)*: Compound **2b** was prepared according to the general procedure. The residue was purified with a mixture of low-boiling petroleum ether/CH_2Cl_2 (3:2) with LiBr and then LiBr/THF as the eluents (R_f = 0.15) to afford **2b** as a brown solid (81 mg, 54 %). ^{1}H NMR (250 MHz, [D$_8$]THF/LiBr; 50 °C): δ = 10.12 (s, 1H; −NH), 9.01 (s, 2H; Ar−H), 8.51 (br s, 4H; Ar−H), 8.42 (br s, 2H; Ar−H), 8.33 (br s, 4H; Ar−H), 8.03 (br s, 1H; −NH), 7.78 (d, ^3J(H,H) = 7.2 Hz, 2H; Ar−H), 7.41 (t, ^3J(H,H) = 7.9 Hz, 2H; Ar−H), 7.24 (t, ^3J(H,H) = 7.5 Hz, 1H; Ar−H), 5.50 (s, 1H; *t*-CH), 3.14–3.05 (m, 10H; α-CH_2), 1.23–2.05 (m, 65H; −CH, −CH_2), 0.93–0.97 ppm (m, 33H; −CH_3); ^{13}C NMR (125 MHz, [D$_8$]THF/LiBr, 50 °C): δ = 157.1, 147.2, 140.6, 140.1, 139.9, 139.7, 130.9, 130.4, 130.3, 130.2, 129.9, 129.1, 127.3, 127.1, 123.7, 123.6, 123.5, 122.5, 121.6, 121.5, 121.3, 120.9, 119.9, 119.5, 119.2, 119.1, 113.8, 50.5, 41.1, 40.9, 40.8, 40.5, 38.5, 35.9, 35.7, 35.6, 34.4, 34.34, 30.5, 29.0, 23.2, 23.1, 20.4 ppm; MS (MALDI-TOF, TCNQ): *m*/*z* (%): 1386 (100 %) [*M*]$^+$.

2,11-Bis-{*N*′-[3,4,5-tris-(dodecyloxyphenyl)ureido]-4-phenyl-1-ethylnyl}-5,8,14,17-tetradodecanylhexa-*peri*-hexabenzocoronene (3): Compound **7** (109 mg, 0,08 mmol), **8** (152 mg, 0,19 mmol), [Pd(PPh$_3$)$_4$] (18 mg, 0,02 mmol), CuI (6 mg, 0,03 mmol) and LiBr (100 mg) were dissolved in a mixture of Et_3N/THF (2:1, 15 mL). The mixture was carefully degassed twice by freeze-thaw method and the reaction lasted for 4 days at 50 °C under argon atmosphere. After it was cooled to room temperature, the reaction was quenched with water (30 mL). The organic phase was extracted with CH_2Cl_2 (3 × 50 mL) and dried over $MgSO_4$. The solvent was removed in vacuo and the product was purified by column chromatography by using THF/CH_2Cl_2 (3:1) with LiBr as the eluent to afford **3** as a yellow powder (81 mg, 13 %). ^{1}H NMR (500 MHz, [D$_8$]THF/LiBr, 50 °C): δ = 8.53 (s, 4H; Ar−H), 8.22–8.01 (m, 12H; Ar−H), 7.72 (d, 4H; ^3J(H,H) = 7 Hz, 4H; Ar−H), 7.51 (d, 4H; ^3J(H,H) = 7 Hz, 4H; Ar−H), 6.82 (s, 4H; Ar−H), 3.91 (t, ^2J(H,H) = 6 Hz, 12H; −OCH_2), 2.89 (br s, 8H; α-CH_2), 1.56–1.30 (m, 180H; −CH_2), 0.92–0.87 ppm (m, 50H; −CH_2, −CH_3); ^{13}C NMR (125 MHz, [D$_8$]THF/LiBr, 50 °C)): δ = 166.0, 159.5, 151.7, 140.8, 138.6, 135.8, 133.9, 133.7, 133.1, 123.2, 118.3, 116.51, 116.47, 114.6, 114.5, 114.2, 113.8, 113.0, 112.8, 112.6, 109.3, 107.3, 106.2, 60.1, 33.0, 32.7, 30.6, 27.9, 26.4, 25.0, 22.7, 21.2, 18.1, 18.0, 15.3, 15.2, 12.5 ppm; MS (MALDI-TOF, TCNQ): *m*/*z* (%): 2770 (100 %) [*M*]$^+$.

Acknowledgements

This work was supported by the EU Integrated Project NAIMO (No. NMP4-CT-2004-500355). We are grateful to Dr. Daniel Wasserfallen and Dr. Xiaoyin Yang for their valuable help and discussions in the preparation of the manuscript.

[1] a) M. O. Sinnokrot, C. D. Sherrill, *J. Am. Chem. Soc.* **2004**, *126*, 7690–7697; b) C. A. Hunter, J. K. M. Sanders, *J. Am. Chem. Soc.* **1990**, *112*, 5525–5534.
[2] a) J. M. Tour, *Chem. Rev.* **1996**, *96*, 537–554; b) M. Müller, C. Kübel, K. Müllen, *Chem. Eur. J.* **1998**, *4*, 2099–2109.
[3] J. W. Steed, J. L. Atwood, *Supramolecular Chemistry,* Wiley, Chichester, **2000**, pp. 22–28.
[4] M. A. B. Bloc, C. Kaiser, A. Khan, S. Hecht, *Topics in Current Chemistry: Functional Molecular Nanostructures* (Ed.: D. Schlüter), Springer, Dordrecht, **2005**.
[5] a) P. Terech, R. G. Weiss, *Chem. Rev.* **1997**, *97*, 3133–3160; b) D. J. Abdallah, R. G. Weiss, *Adv. Mater.* **2000**, *12*, 1237–1247; c) F. Camerel, R. Ziessel, B. Donnio, C. Bourgogne, D. Guillon, M. Schmutz, C. Iacovita, J.-P. Bucher, *Angew. Chem.* **2007**, *119*, 2713–2716; *Angew. Chem. Int. Ed.* **2007**, *46*, 2659–2662 .
[6] H. Engelkamp, S. Middelbeek, R. J. M. Nolte, *Science* **1999**, *284*, 785–788.
[7] S. Shinkai, K. Murata, *J. Mater. Chem.* **1998**, *8*, 485–495.
[8] A. M. van de Craats, J. M. Warman, K. Müllen, Y. Geerts, J. D. Brand, *Adv. Mater.* **1998**, *10*, 36–38.
[9] C. D. Dimitrakopoulos, P. R. L. Malenfant, *Adv. Mater.* **2002**, *14*, 99–117.
[10] a) J. H. Burroughes, D. D. C. Bradley, A. R. Brown, R. N. Marks, K. Mackay, R. H. Friend, P. L. Burns, A. B. Holmes, *Nature* **1990**, *347*, 539–541; b) R. H. Friend, R. W. Gymer, A. B. Holmes, J. H. Burroughes, R. N. Marks, C. Taliani, D. D. C. Bradley, D. A. Dos Santos, J. L. Brédas, M. Lögdlund, W. R. Salaneck, *Nature* **1999**, *397*, 121–128.

[11] L. Schmidt-Mende, A. Fechtenkötter, K. Müllen, E. Moons, R. H. Friend, J. D. MacKenzie, *Science* **2001**, *293*, 1119–1122.

[12] a) W. Pisula, A. Menon, M. Stepputat, I. Lieberwirth, U. Kolb, A. Tracz, H. Sirringhaus, T. Pakula, K. Müllen, *Adv. Mater.* **2005**, *17*, 684–689; b) S. Kubowicz, U. Pietsch, M. D. Watson, N. Tchebotareva, K. Müllen, A. F. Thünemann, *Langmuir* **2003**, *19*, 5036–5041; c) D. W. Breiby, O. Bunk, W. Pisula, T. I. Sølling, A. Tracz, T. Pakula, K. Müllen, M. M. Nielsen, *J. Am. Chem. Soc.* **2005**, *127*, 11288–11293.

[13] a) J. Wu, A. Fechtenkötter, J. Gauss, M. D. Watson, M. Kastler, C. Fechtenkötter, M. Wagner, K. Müllen, *J. Am. Chem. Soc.* **2004**, *126*, 11311–11321; b) J. Wu, M. D. Watson, N. Tchebotareva, Z. Wang, K. Müllen, *J. Org. Chem.* **2004**, *69*, 8194–8204; c) M. Kastler, W. Pisula, D. Wasserfallen, T. Pakula, K. Müllen, *J. Am. Chem. Soc.* **2005**, *127*, 4286–4296.

[14] a) C. D. Simpson, J. Wu, M. D. Watson, K. Müllen, *J. Mater. Chem.* **2004**, *14*, 494–504; b) J. Wu, M. Baumgarten, M. G. Debije, J. M. Warman, K. Müllen, *Angew. Chem.* **2004**, *116*, 5445–5449; *Angew. Chem. Int. Ed.* **2004**, *43*, 5331–5335; c) A. M. van de Craats, N. Stutzmann, O. Bunk, M. M. Nielsen, M. D. Watson, K. Müllen, H. D. Chanzy, H. Sirringhaus, R. H. Friend, *Adv. Mater.* **2003**, *15*, 495–499.

[15] D. Wasserfallen, I. Fischbach, N. Chebotareva, M. Kastler, W. Pisula, F. Jäckel, M. D. Watson, I. Schnell, J. P. Rabe, H. W. Spiess, K. Müllen, *Adv. Funct. Mater.* **2005**, *15*, 1585–1594.

[16] a) L. J. Prins, D. N. Reinhoudt, P. Timmerman, *Angew. Chem.* **2001**, *113*, 2446–2492; *Angew. Chem. Int. Ed.* **2001**, *40*, 2382–2426; b) K. J . C. van Bommel, A. Friggeri, S. Shinkai, *Angew. Chem.* **2003**, *115*, 1010–1030; *Angew. Chem. Int. Ed.* **2003**, *42*, 980–999.

[17] a) M. Shirakawa, S. Kawano, N. Fujita, K. Sada, S. Shinkai, *J. Org. Chem.* **2003**, *68*, 5037–5044; b) J. J. van Gorp, J. A. J. M. Vekemans, E. W. Meijer, *J. Am. Chem. Soc.* **2002**, *124*, 14759–14769; c) S.-i. Tamaru, M. Nakamura, M. Takeuchi, S. Shinkai, *Org. Lett.* **2001**, *3*, 3631–3634; d) K. Sugiyasu, N. Fujita, S. Shinkai, *Angew. Chem.* **2004**, *116*, 1249–1253; *Angew. Chem. Int. Ed.* **2004**, *43*, 1229–1233.

[18] a) S. Ito, M. Wehmeier, J. D. Brand, C. Kübel, R. Epsch, J. P. Rabe, K. Müllen, *Chem. Eur. J.* **2000**, *6*, 4327–4342; b) A. Fechtenkötter, N. Tchebotareva, M. D. Watson, K. Müllen, *Tetrahedron* **2001**, *57*, 3769–3783.

[19] J. Zhang, G. Podoprygorina, V. Brusko, V. Böhmer, A. Janshoff, *Chem. Mater.* **2005**, *17*, 2290–2297.

[20] a) W. J. Schutte, M. Sluyters-Rehbach, J. H. Sluyters, *J. Phys. Chem.* **1993**, *97*, 6069–6073; b) K. Kano, K. Fukuda, H. Wakami, R. Nishiyabu, R. F. Pasternack, *J. Am. Chem. Soc.* **2000**, *122*, 7494–7502; c) A. Tracz, J. K. Jeszka, M. D. Watson, W. Pisula, K. Müllen, T. Pakula, *J. Am. Chem. Soc.* **2003**, *125*, 1682–1683.

[21] F. J. M. Hoeben, P. Jonkheijm, E. W. Meijer, A. P. H. J. Schenning, *Chem. Rev.* **2005**, *105*, 1491–1546.

[22] R. B. Prince, J. G. Saven, P. G. Wolynes, J. S. Moore, *J. Am. Chem. Soc.* **1999**, *121*, 3114–3121.

[23] E. Clar, *Polycyclic Hydrocarbons,* Academic Press, New York, **1964**.

[24] a) F. Dörr, *DMS UV ATLAS of Organic Compounds, Vol. III*, Verlag Chemie, Weinheim; Butterworths, London, **1966**, p. E1; b) J. Beier, PhD Thesis, University of Bayreuth (Germany), **2000**, pp. 50–62.

[25] a) R. M. Silverstein, G. C. Bassler, T. C. Morrill, *Spectrometric Identification of Organic Compounds,* 5th ed., Wiley, **1991**, p. 122; b) N. B. Colthup, L. H. Daly, S. E. Wiberley, *Introduction to Infrared and Raman Spectroscopy,* 3rd ed., Academic Press, New York, **1990**, p. 320.

[26] DSC experiments were performed from −100 to 250 °C with a heating/cooling rate of 10 °C min^{-1}.

[27] 2D WAXS experiments were performed with the fibers that were mechanically extruded at 150 °C; for details, see: a) I. Fischbach, T. Pakula, P. Minkin, A. Fechtenkötter, K. Müllen, H. W. Spiess, *J. Phys. Chem. B* **2002**, *106*, 6408–6418; b) W. Pisula, Z. Tomovic, C. Simpson, M. Kastler, T. Pakula, K. Müllen, *Chem. Mater.* **2005**, *17*, 4296–4303.

[28] S. Chandrasekhar, B. K. Sadashiva, K. A. Suresh, *Pramana* **1977**, *9*, 471–480.

[29] The inverted gel was slowly heated in a water bath from 25 °C with a speed of 0.5 °C min^{-1}. The temperature at which the gel started to flow was recorded as T_g.

[30] The xerogels were prepared by dropping the gel formed onto a precleaned silicon wafer under the corresponding solvent atmosphere and the solvent was slowly evaporated.

[31] a) J. Coril, D. A. Dos Santos, D. Beljonne, Z. Shuai, J. L. Brédas in *Semiconducting Polymers* (Eds.: G. Hadziioannou, P. F. van Hutten), Wiley-VCH, Weinheim, **2000**, p. 88; b) F. D. Lewis, T. Wu, E. L. Burch, D. M. Bassani, J.-S. Yang, S. Schneider, W. Jäger, R. L. Letsinger, *J. Am. Chem. Soc.* **1995**, *117*, 8785–8792; c) K. Liang, M. S. Farahat, J. Perlstein, K.-Y. Law, D. G. Whitten, *J. Am. Chem. Soc.* **1997**, *119*, 830–831.

[32] a) G. A. Jeffrey, *An Introduction to Hydrogen Bonding,* Oxford University Press, Oxford, **1997**; b) S. H. Gellman, G. P. Dado, G. B. Liang, B. R. Adams, *J. Am. Chem. Soc.* **1991**, *113*, 1164–1173; and references therein.

[33] a) S. Kawano, S. Tamaru, N. Fujita, S. Shinkai, *Chem. Eur. J.* **2004**, *10*, 343–351; b) H. J. Tian, K. Inoue, K. Yoza, T. Ishi-i, S. Shinkai, *Chem. Lett.* **1998**, 871–872; c) L. Lu, M. Cocker, R. E. Bachman, R. G. Weiss, *Langmuir*, **2000**, *16*, 20–34.

[34] a) K. Hanabusa, C. Koto, M. Kimura, H. Shirai, A. Kakehi, *Chem. Lett.* **1997**, 429–430; b) R. I. Gearba, M. Lehmann, J. Levin, D. A. Ivanov, M. H. J. Koch, J. Barberá, M. G. Debije, J. Piris, Y. H. Geerts, *Adv. Mater.* **2003**, *15*, 1614–1618.

[35] a) X. Zhao, Y. L. Chang, F. W. Fowler, J. W. Lauher, *J. Am. Chem. Soc.* **1990**, *112*, 6627–6634; b) M. C. Etter, Z. Urbanczyk-Lipkowska, M. Zia-Ebrahimi, T. W. Panunto, *J. Am. Chem. Soc.* **1990**, *112*, 8415–8426; c) J. H. van Esch, S. De Feyter, R. M. Kellogg, F. De Schryver, B. L. Feringa, *Chem. Eur. J.* **1997**, *3*, 1238–1243; d) L. E. Orgel, *Rev. Mod. Phys.* **1959**, *31*, 100–102; e) M. L. Bushey, A. Hwang, P. W. Stephens, C. Nuckolls, *Angew. Chem.* **2002**, *114*, 2952–2955; *Angew. Chem. Int. Ed.* **2002**, *41*, 2828–2831; f) M. P. Lightfoot, F. S. Mair, R. G. Pritchard, J. E. Warren, *Chem. Commun.* **1999**, 1945–1946; g) S. Tamaru, S. Uchino, M. Takeuchi, M. Ikeda, T. Hatano, S. Shinkai, *Tetrahedron Lett.* **2002**, *43*, 3751–3755.

[36] a) J. P. Hill, W. Jin, A. Kosaka, T. Fukushima, H. Ichihara, T. Shimomura, K. Ito, T. Hashizume, N. Ishii, T. Aida, *Science* **2004**, *304*, 1481–1483; b) W. Jin, T. Fukushima, M. Niki, A. Kosaka, N. Ishii, T. Aida, *Proc. Natl. Acad. Sci. U.S.A.* **2005**, *102*, 10801–10806.

[37] F. Würthner, B. Hanke, M. Lysetska, G. Lambright, G. S. Harms, *Org. Lett.* **2005**, *7*, 967–970.

[38] a) V. K. Praveen, S. J. George, R. Varghese, C. Vijayakumar, A. Ajayaghosh, *J. Am. Chem. Soc.* **2006**, *128*, 7542–7550; b) F. S. Schoonbeek, J. H. van Esch, B. Wegewijs, D. B. A. Rep, M. P. de Haas, T. M. Klapwijk, R. M. Kellogg, B. L. Feringa, *Angew. Chem.* **1999**, *111*, 1486–1490; *Angew. Chem. Int. Ed.* **1999**, *38*, 1393–1397; ; c) N. Mizoshita, Y. Suzuki, K. Kishimoto, K. Hanabusa, T. Kato, *J. Mater. Chem.* **2002**, *12*, 2197–2201; d) N. M. Sangeetha, U. Maitra, *Chem. Soc. Rev.* **2005**, *34*, 821–836.

Received: June 17, 2007
Published online: October 8, 2007

